

# **Mg Magnesium Technology 2012**

**Alloy and Microstructural Design**  
**Wednesday AM**

***Session Chairs:***

**Jian-Feng Nie**  
**(Monash University, Australia)**

**Nack Kim**  
**(POSTECH, South Korea)**

## Age hardening behavior of Mg-1.2Sn-1.7Zn alloy containing Al

T. T. Sasaki, T. Ohkubo, K. Hono

National Institute for Materials Science, 1-2-1 Sengen, Tsukuba, Ibaraki, 305-0047, Japan

Keywords: Mg-Sn, Precipitation hardening, Al

### Abstract

We have investigated the age hardening behavior of Mg-1.2at.%Sn (T5) based alloys, which are solution treatable at lower temperature as compared to the previously studied Mg-2.2Sn (T10) based alloys. To enhance the age hardening response with the reduced Sn content, Zn and Al were alloyed with the Mg-1.2at.%Sn alloy. Particularly, Mg-1.7Zn-1.2Sn-2.0Al alloy (TZA543) showed the peak hardness of 79 VHN at 200°C. The peak aged Mg-1.2Sn-1.7Zn-2.0Al alloy consisted of cuboidal  $\beta_2'$  precipitates with the size of less than 50 nm, rod shaped precipitates, and lathplate shaped  $Mg_2Sn$  phase.

### Introduction

There are strong demands for the development of high strength wrought magnesium alloys applicable to transportation vehicles and aircrafts. Since commercial wrought alloys such as Mg-Zn-Zr (ZK) and Mg-Al-Zn (AZ) show only moderate age hardening responses, not much attention has been paid to the precipitation hardening of wrought alloys. Recent investigations showed yield strength can be readily increased by aging rolled sheets and extruded rods of microalloyed Mg-Zn alloys microalloyed with Ca and Ag [1], demonstrating the potential of heat treatable wrought magnesium alloys.

Mg-Sn based alloys appear to be promising as heat resistant alloys for both cast and wrought applications because the  $Mg_2Sn$  phase has a higher melting temperature than those in Mg-RE (RE: Rare Earth) systems [2]. In fact, some of precipitation hardened Mg-Sn based alloys exhibit excellent creep properties [3, 4]. For better formability, extrusion and rolling temperature should be selected above the solvus temperature of alloys. However, the solution heat treatment temperature of the previously studied Mg-2.2Sn based alloy (>500 °C) is too high for thermomechanical processing [5]. One way to reduce the solution treatment temperature is to decrease the Sn content. However, it also reduces the age hardening responses. Since the typical size of  $Mg_2Sn$  precipitates is rather coarse (~1  $\mu m$ ) [5-8], the significant refinement of the precipitates may compensate the degradation of the age hardening response even with the reduced supersaturation. In Mg-Sn-Zn alloys,  $MgZn_2$  type phase such as  $\beta_1'$  phase provides the heterogeneous nucleation site for the  $Mg_2Sn$  phase [8, 9], thereby increasing the number density of the  $Mg_2Sn$  precipitates. In this work, 1.7at.%Zn was alloyed with Mg-1.2at.%Sn so that the alloy can be solution treated at 450 °C. Since the addition of Al is reported to refine the  $Mg_2Sn$  phase in the Mg-2.2Sn-0.5at.%Zn alloy [8, 10], we examined the effect of Al alloying expecting the improvement of the age hardening behavior of the Mg-1.2at.%Sn-1.7at.%Zn alloy (TZ54).

### Experimental Procedure

Alloy ingots with nominal compositions of Mg-1.2Sn-1.7Zn-xAl (x=0, 0.5, 1 and 2) in at.% were prepared by induction melting using steel crucibles under an Ar atmosphere and by casting into iron moulds. Table 1 shows the compositions of the alloys in both at.% and wt.%.

Table 1: Chemical composition of alloys

at.%	wt.%
Mg-1.2Sn-1.7Zn	Mg-5.5Sn-4.3Zn
Mg-1.2Sn-1.7Zn-0.5Al	Mg-5.4Sn-4.3Zn-0.5Al
Mg-1.2Sn-1.7Zn-1.0Al	Mg-5.4Sn-4.2Zn-1.0Al
Mg-1.2Sn-1.7Zn-2.0Al	Mg-5.4Sn-4.2Zn-2.1Al

The ingots were subjected to homogenization at 350 °C for 24 hr followed by 450 °C heat treatment for 24 hr in a He-filled Pyrex tube. The small samples that were cut out from the ingots were solution heat treated for 0.5 hr s at 450 °C in the He-filled Pyrex tubes and then water quenched. Single aging was performed on alloys at 200 °C in an oil bath for various aging times. The age hardening responses were measured by the Vickers hardness tester under a load of 500 g. Transmission electron microscope (TEM) specimens were prepared by the twin-jet polishing technique using a solution of 5.3 g LiCl, 11.16 g  $Mg(ClO_4)_2$ , 2,500 ml methanol, and 100ml 2-butoxy-ethanol at about -50 °C and 90 V. Some of the specimens were finished for surface cleaning by ion milling using a Gatan Precision Ion Polishing System (PIPS). Transmission Electron Microscope (TEM) observation was carried out using FEI TECNAI T20 TEM operating at 200 kV.

### Results and Discussion

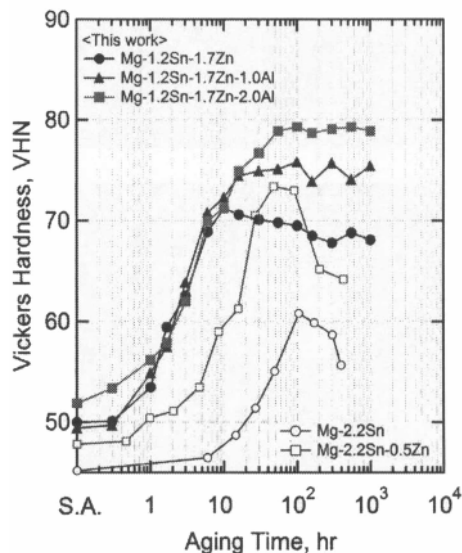


Figure 1: Variation in Vickers Hardness as functions of time during aging at 200°C on Mg-1.2Sn-1.7Zn, Mg-1.2Sn-1.7Zn-1.0Al and Mg-1.2Sn-1.7Zn-2.0Al alloys. Included is the data obtained from Mg-2.2Sn and Mg-2.2Sn-0.5Zn alloy [5].

**Figure 1** shows variations in Vickers hardness as functions of time during 200 °C aging for Mg-1.2Sn-1.7Zn (TZ54), Mg-1.2Sn-1.7Zn-1.0Al (TZ541) and Mg-1.2Sn-1.7Zn-2.0Al (TZ542) alloys. The age hardening curves show that the addition of Al substantially increased the peak hardness. The peak hardness increased from 71 to 79 VHN by the addition of 2at.% Al while the time to reach the peak hardness is delayed by the Al addition. Mg-1.2Sn-1.7Zn alloy reached the peak hardness after 10 h of aging at 200 °C, and Mg-1.2Sn-1.7Zn-2.0Al alloy took 100 h to reach the peak hardness. While Harosh et al. reported two hardness peaks appeared in an Mg-5.6Sn-4.4Zn-2.1Al alloy during aging at 225 °C [11], the Mg-1.2Sn-1.7Zn-2.0Al alloy showed only one hardness peak. The Mg-1.2Sn-1.7Zn based alloys do not overage as quickly as Mg-2.2Sn and Mg-2.1Sn-0.5Zn alloys [5]. The Mg-1.2Sn-1.7Zn alloy maintained the peak hardness of ~ 70 VHN up to 100 h and the Mg-1.2Sn-1.7Zn-2.0Al alloy maintained the hardness level of ~ 80 VHN up to 1000 h during 200 °C aging.

**Figure 2** shows the bright field TEM images obtained from the Mg-1.2Sn-1.7Zn alloy aged at 200 °C. **Figure 2 (a) and (b)** are those after aging at 200°C for 10 h, which corresponds to the peak aged condition, and **Fig. 2 (c) and (d)** are the ones after overaging for 100 h at 200 °C. Note that **Fig. 2 (a) and (c)** are

taken from the  $[11\bar{2}0]$  zone, and **Fig. 2 (b) and (d)** are from the  $[0001]$  zone, respectively. As shown in **Fig. 2 (a) and (b)**, the peak aged Mg-1.2Sn-1.7Zn alloy shows similar microstructure to that seen in the Mg-Zn based alloy subjected to aging [12, 13], i.e., rod shaped  $\beta_1'$  along the  $[0001]$  direction of the magnesium matrix, and the other is  $\beta_2'$  plates lying on the  $(0001)$  plane of the magnesium matrix. The corresponding SAED pattern in **Fig. 2 (a)** exhibits diffuse streaks along the  $[01\bar{1}0]$  directions. This is attributed to the rod shaped  $\beta_1'$  precipitates along the  $[0001]$  direction as well as the crystal structure of the precipitate phase.

The overaging for 100 h resulted in the coarsening of the  $\beta_1'$  and  $\beta_2'$  phases as shown in **Fig. 2 (c) and (d)**. The  $\beta_1'$  phase coarsened to ~ 1  $\mu\text{m}$  in length and 40 nm in diameter, and the size of the  $\beta_2'$  phase increased to 200 nm in diameter and 50 nm in thickness. In addition to the coarsened  $\beta_1'$  and  $\beta_2'$  phases, another kind of precipitates is observed as indicated by an arrow. From **Fig. 2 (c) and (d)**, the precipitates have plate like shape forming on the prismatic plane of the magnesium matrix,  $(10\bar{1}0)$ .

**Figure 3 (a)** shows the microbeam diffraction patterns obtained from one of the plate like precipitates. Note that they are recorded from the  $[01\bar{1}0]$  zone. The precipitates are identified as the

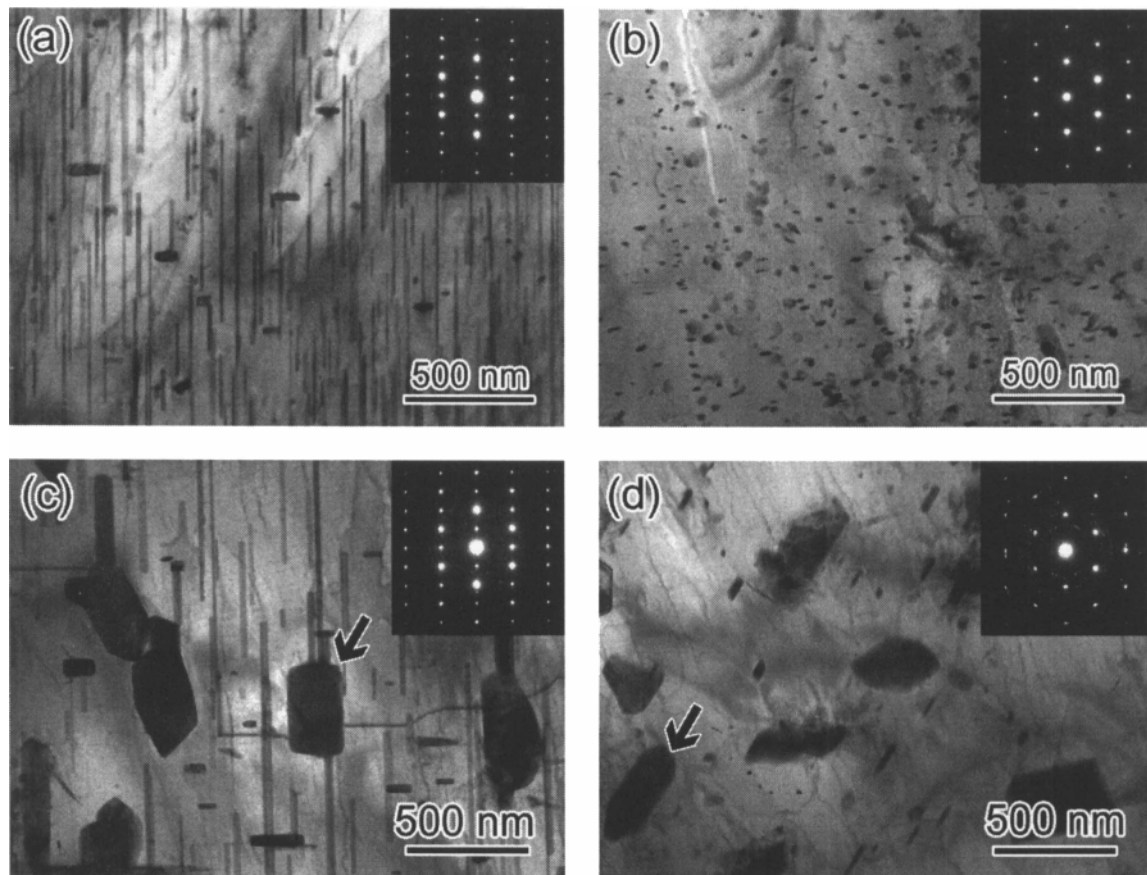


**Figure 2:** Bright field TEM images of Mg-1.2Sn-1.7Zn alloy subjected to 200 °C aging. (a) and (b) are obtained after 200°C/10hr aging, which is consistent with the peak aging condition, and (c) and (d) are obtained after aging at 200°C for 100hr. (a) and (c) are taken from the zone axis of  $[11\bar{2}0]$ , and (b) and (d) are taken from the zone axis of  $[0001]$ .

Mg<sub>2</sub>Sn phase as shown in the calculated diffraction pattern, Fig. 3 (b). The orientation relationship (OR) between the plate like Mg<sub>2</sub>Sn phase forming on the prismatic and the magnesium matrix is determined to be  $(0001)_{Mg} // (110)_{Mg_2Sn}$ ,  $[11\bar{2}0]_{Mg} // [001]_{Mg_2Sn}$ , which is the common OR in the Mg-Sn based alloy [5-8]. The late precipitation of Mg<sub>2</sub>Sn phase after the peak aged condition is considered to compensate the hardness drop due to the coarsening of the  $\beta_1'$  and  $\beta_2'$  phases.

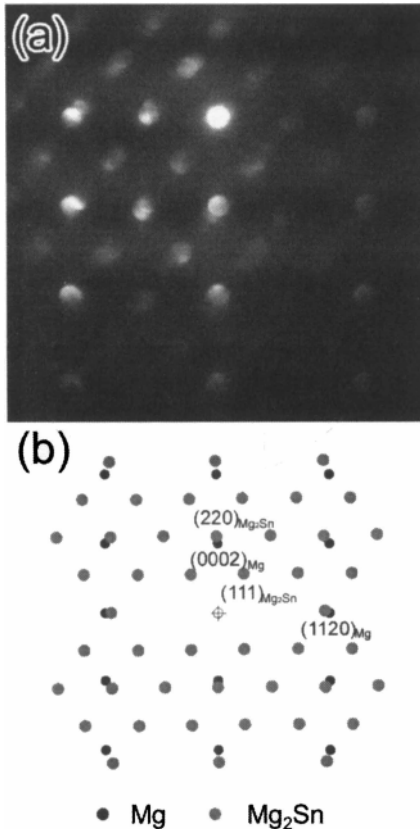


**Figure 3:** (a) microbeam diffraction patterns obtained from a precipitate indicated by arrow in Fig. 2 (a), and (b) Calculated diffraction patterns. Note that these images are taken from the zone axis of  $[01\bar{1}0]$ .

**Figure 4** shows the bright field TEM images obtained from the Mg-1.2Sn-1.7Zn-2.0Al alloy (TZA542) aged at 200 °C for 100 hr, which corresponds to the peak aged condition. Note that **Fig. 4 (a) and (b)** are taken from the  $[11\bar{2}0]$ , and  $[0001]$  zones, respectively. The peak aged microstructure shows different feature as compared to the peak aged Mg-1.2Sn-1.7Zn alloy. The rod shaped precipitate growing along  $[0001]$  direction is refined to ~ 300 nm as indicated by arrowhead 1. In addition, as reported by Oh-ishi et al. [10], the Al addition resulted in the formation of the cuboidal shaped precipitates with the size less than 50 nm as indicated by arrowhead 2. In addition to these precipitates, the lath shaped precipitates forming on the prismatic plane could be also observed as indicated by arrowhead 3. The lath shaped precipitates are the Mg<sub>2</sub>Sn phase, and its size was refined to ~200 nm in length and ~75 nm in thickness.

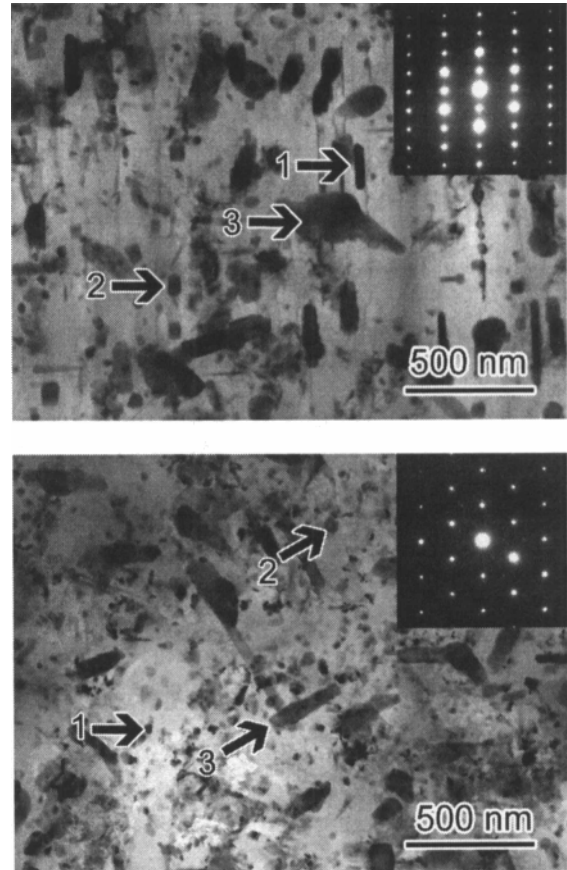


**Figure 4:** Bright field TEM images of Mg-1.2Sn-1.7Zn-2.0Al alloy aged at 200 °C aging for 100 hr, consistent with the peak aging condition. (a) and (b) are taken from the zone axis of  $[11\bar{2}0]$ , and  $[0001]$ , respectively.

**Figure 5 (a)** shows the micro-beam diffraction pattern obtained from the cuboidal precipitates observed in the 200 °C / 100 hr aged Mg-1.2Sn-1.7Zn-2.0Al alloy taken from the zone axis of  $[0001]$ . As shown in **Fig. 5 (b)**, the structure of the cuboidal precipitate is consistent with that of the  $\beta_2'$  phase. However, since the structure of the rod precipitates remains unclear, future work will shed light on the clarification of the phase of the rod shaped precipitates.

In this work, we have investigated the age hardening behavior of Mg-1.2Sn-1.7Zn based alloy containing Al, and found that the peak hardness of the Mg-1.2Sn-1.7Zn based alloy could be substantially increased from 71 to 79 VHN by the addition of 2.0at.% of Al. From the microstructure observation of the Mg-2.1Sn-1.7Zn alloy at peak aged and over aged conditions, **Fig. 2**, the peak hardness was attributed to the precipitation of the  $\beta_1'$  and  $\beta_2'$  phases, **Fig. 2 (a) and (b)**. Although the hardness is expected to decrease upon the coarsening of the  $\beta_1'$  and  $\beta_2'$  phases by the over aging, the Mg-1.2Sn-1.7Zn based alloys showed smaller hardness reduction up to 1000 h. This is because Mg<sub>2</sub>Sn phase precipitated after the peak aging, and could compensate the hardness decrease due to the coarsening of the  $\beta_1'$  and  $\beta_2'$  phases, **Fig. 2 (c) and (d)**. Since the diffusion of the Sn atoms is much

slower as compared to that of the Zn atoms in the magnesium matrix, and Zn and Sn atoms behave repulsively due to the positive enthalpy of mixing as reported previously [5, 14], we can understand the precipitation of the  $\beta_1'$  and  $\beta_2'$  phases prior to the precipitation of the  $Mg_2Sn$  phase.

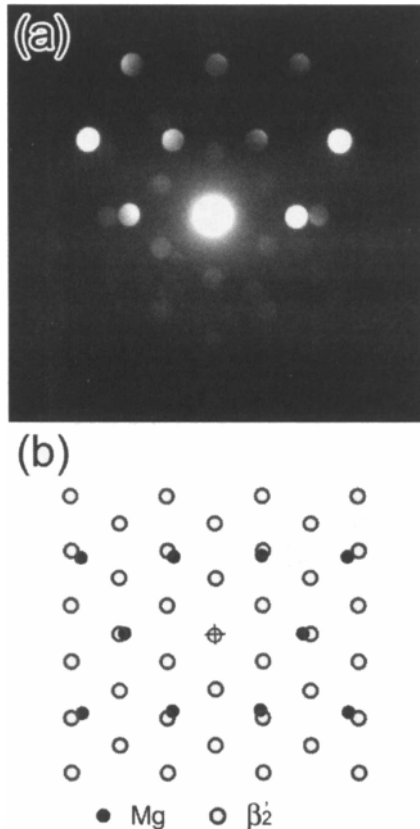


**Figure 5:** (a) microbeam diffraction patterns obtained from one of cuboidal precipitate seen in 200°C/100hr aged Mg-1.2Sn-1.7Zn-2.0Al alloy, and (b) Calculated diffraction patterns. Note that these images are taken from the zone axis of  $[10\bar{1}0]$ .

In the Mg-1.2Sn-1.7Zn-2.0Al alloy, on the other hand, the  $Mg_2Sn$  phase also contributes to the peak hardness in addition to the rod shaped and cuboidal shaped precipitates as seen in Fig. 4. The precipitation of the  $Mg_2Sn$  resulted in the increased number density of the precipitates in the peak aged condition, resulting in the enhanced peak hardness in the Mg-1.2Sn-1.7Zn-2.0Al alloy. The time to reach peak hardness was shortened in the Mg-2.2Sn-0.5Zn alloy even by the addition of 1.0at.% Al [8]. The presence of the  $Mg_2Sn$  phase in the peak aged condition is attributed to the change in the kinetics due to the Al.

The enhanced peak hardness in the Mg-1.2Sn-1.7Zn-2.0Al alloy is also attributed to the increase in the number density of the precipitates, and the change in the morphology of the precipitates. The addition of Al refined the precipitate size as shown in the microstructure of the peak aged samples, Fig. 2 and 4. The peak aged Mg-1.2Sn-1.7Zn-2.0Al alloy consisted of fine cuboidal  $\beta_2'$  precipitates with the size of less than 50 nm, rods

along  $[0001]$ , and fine plate shaped  $Mg_2Sn$  phase while the Mg-1.2Sn-1.7Zn alloy was mainly strengthened by coarse rod shaped  $\beta_1'$  phase with over 500 nm in length. In the Mg-2.3Zn-0.5Mn alloy, Oh-ishi et al concluded that plate to cuboidal transition of  $\beta_2'$  phase is because of the lattice misfit change between the Mg and precipitate phases by Al addition [10]. This may also have caused the shape changes of the precipitates in this system.

Finally, the  $Mg_2Sn$  phase observed in the Mg-1.2Sn-1.7Zn had different shape from the ones seen in the previously studied Mg-Sn based alloy [5-9]. The plate like precipitates forming on the prismatic plane of the magnesium matrix,  $(11\bar{2}0)$  could be observed, Fig. 2 (c) and (d), while the  $Mg_2Sn$  phase usually forms on the  $(0001)$  plane of the magnesium matrix [5-9]. Since the precipitation of the  $Mg_2Sn$  on the prismatic plane could be seen even in the Al-free Mg-1.2Sn-1.7Zn alloy, the lattice misfit change due to Al addition might not be the sole reason for the precipitation on the prismatic plane. Therefore, future work will also shed light on the detailed formation mechanism of the  $Mg_2Sn$  phase.

### Summary

We have investigated the age hardening behavior of the Mg-1.2Sn-1.7Zn-xAl ( $x=0.5, 1.0$  and  $2.0$ ). The addition of 2.0at.%Al substantially increased the peak hardness from 71 to 79 VHN while the time to reach peak hardness was delayed. In the Mg-1.2Sn-1.7Zn alloy, the peak hardness is attributed to the precipitation of  $\beta_1'$  and  $\beta_2'$  phases. On the other hand, the refinement of the rod precipitates along  $[0001]$  direction and the precipitation of fine cuboidal  $\beta_2'$  phase and  $Mg_2Sn$  phase resulted in the increase in the peak hardness in the Mg-1.2Sn-1.7Zn-2.0Al alloy.

### Acknowledgement

The authors gratefully acknowledge Dr. C. L. Mendis for her fruitful discussion.

### References

- [1] C.L. Mendis, K. Oh-ishi, Y. Kawamura, T. Honma, S. Kamado, K. Hono, "Precipitation-hardenable Mg-2.4Zn-0.1Zn-0.1Ca-0.16 Zr (at.%) alloys," *Acta Materialia*, 57 (3) (2009) 749-760.
- [2] A.A. Nayeb-Hashemi and J.B. Clark, *Phase Diagrams of Binary Magnesium Alloys*, (Materials Park, OH ASM International, 1988).
- [3] M.A. Gibson, X. Fang, C.J. Bettles, C.R. Hutchinson, "The effect of precipitate state on the creep resistance of Mg-Sn alloys," *Scripta Materialia*, 63 (8) (2010) 899-902.
- [4] T.T. Sasaki, T. Ohkubo, K. Hono, "Heat-treatable Mg-Sn-Zn wrought alloy," *Scripta Materialia*, 61 (1) (2009) 80-83
- [5] T.T. Sasaki, K. Oh-ishi, T. Ohkubo, K. Hono, "Enhanced age hardening response by the addition of Zn in Mg-Sn alloys," *Scripta Materialia*, 55 (3) (2006) 251-254.
- [6] C.L. Mendis, C.J. Bettles, M.A. Gibson, C.R. Hutchinson, "An enhanced age hardening response in Mg-Sn based alloy containing Zn" *Materials Science and Engineering A*, 435 (2006) 163-171.
- [7] C.L. Mendis, C.J. Bettles, M.A. Gibson, S. Grosse, C.R. Hutchinson, "Refinement of precipitate distributions in and age-hardenable Mg-Sn alloy through microalloying" *Philosophical Magazine Letters*, 86 (7) (2006) 443-456.
- [8] T.T. Sasaki, K. Oh-ishi, T. Ohkubo, K. Hono, "Effect of double aging and microalloying on the age hardening behavior of

a Mg-Sn-Zn alloy," *Materials Science and Engineering A*, (2011)  
doi: 10.1016/j.msea.2010.05.010.

[9] A. Gorny, A. Katsman, "Precipitation and stress-influenced coarsening in Mg-based Mg-Zn-Sn-Y and Mg-Zn-Sn-Sb alloys" *Journal of Materials Research*, 23 (2008) 1228-1236

[10] K. Oh-ishi, K. Hono, K.S. Shin, "Effect of pre-aging and Al addition on age hardening and microstructure in Mg-6wt.%Zn alloys," *Materials Science and Engineering A*, 496 (2008) 425-433.

[11] S. Harosh, L. Miller, G. Levi, M. Bamberger, "Microstructure and properties of Mg-5.6%Sn-4.4%Zn-2.1%Al alloy," *Journal of Materials Science*, 42 (2007) 9983-9989

[12] J.B. Clark, "Transmission electron microscopy study of age hardening in a Mg-5 wt.%Zn alloy," *Acta Metallurgica*, 13 (12) (1965) 1281.

[13] G. Mima, Y. Tanaka, "The Aging Characteristics of Magnesium-4 wt% Zinc Alloy" *Transactions of Japan Institute of Metals*, 12 (2) (1971) 71-75.

[14] A.B. Eric and G.B. Brook, *Smithells Metals Reference Book*, (7th ed.), (Oxford, Butterworth-Heinemann, 1992)